

Effects of element widths and FOV on SENSE imaging

Dan K. Spence¹, Steven M. Wright¹

¹Department of Electrical Engineering, Texas A&M University

INTRODUCTION:

Since the introduction of SENSE imaging, various groups [1,2] have presented new array topologies in hopes of maximizing the reduction factors as well as the image SNR. The common convention for characterizing a new array topology is to present a g-factor map over the desired FOV, the region the array is intended to function, and list the maximum and mean g-factor over this region. Several questions regarding this convention immediately spring to mind. What trade off in terms of overall array sensitivity was made in order to optimize the g-factor? What is the effect of imaging an object that doesn't correspond to the desired FOV? Is the array truly optimal in terms of g-factor?

Recently, Wiesinger [3] has published results on the ultimate SNR and ultimate g-factor for SENSE imaging, based on "hypothetical 'complete' coil arrays," showing the fundamental limits on SENSE imposed by Maxwell's equations. In this abstract, results are presented showing what can be achieved from four coil and six coil arrays as coil width and desired FOV are varied. The results show the range over which the array has an acceptable g-factor performance. The acceptable range of FOV is dependent up coil positioning and is greatly affected by reduction factor. With respect to the coil width, the best performance, regardless of reduction factor, corresponds with the width that produces an SNR maximum at the center of the FOV. This corroborates the results by Reykowski [4] and Weisinger [3] that the optimal g-factor performance corresponds with optimal SNR performance.

METHODS:

For simplicity, a quasi-static model consisting of infinitely long coils was used. The geometry of the model is shown in figure 1. The coils are positioned on the surface of a cylinder with a radius of 25cm. The sensitivity of each of the coils is computed along a line, 10cm above center, covering the desired field of view for a coronal image. The phase encode direction is chose to be parallel to this line. The mutual resistance between elements is similarly computed with a lossy 20cm square sample, the shaded region, centered on the origin. The coil elements are equally space and the entire array rotated about the origin.

The combined SNR is computed at the center of the field of view. The maximum g-factor along the line is also found for the specified reduction factor. Since the SNR is scaled by the inverse of the g-factor and g-factor is always greater than or equal to one, it seems more appropriate to plot the inverse since it will be constrained between zero and one. This value is recomputed for each array configuration and maps of the g-factor inverse versus coil width and field of view are generated.

RESULTS:

Maps of the g-factor inverse for the four coil array are shown in figure two. In this example a reduction factor of two was used. The graphs cover a span of coil widths from 1.5cm and a span of 1cm to

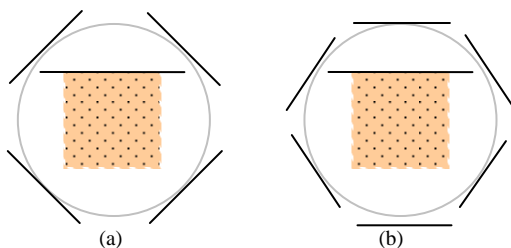


Figure 1: (a) Four element geometry (b) Six element geometry

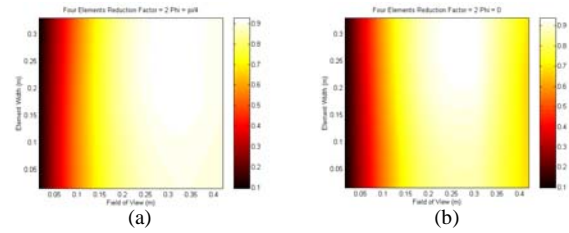


Figure 2: Maps of the inverse of the maximum g-factor as the element width and FOV dimensions are changed for a 4 element array at R=2. The map in (a) is generated by the 4 coil geometry shown in figure 1. In (b), the coil array was rotated by 45 degrees about the origin.

42 cm. In the figure 2a, the coil array is as shown in figure 1a. In 2b, the coil array has been rotated by 45 degrees about the origin. The maximum SNR for the center pixel of the FOV occurs at an element width of 18.5cm. The maximum mean SNR over the FOV occurs at an element width of 25cm in both cases. The minimal g-factor also occurs at this coil width, but is still dependent upon FOV. The optimal FOVs for the arrays are approximately 30cm and 26cm for the un-rotated and rotated cases respectively. However, acceptable values of g-factor still are found over a broad range of FOVs. In practice, the array, as shown in figure 1a, would prove more useful since it has acceptable performance over a broader range of FOV.

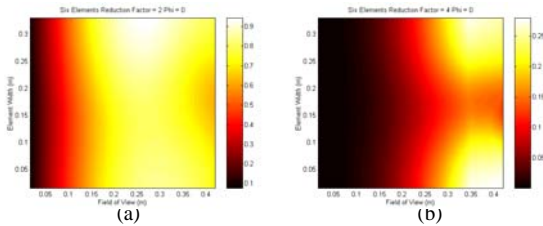


Figure 3: Maps of the inverse of the maximum g-factor in the FOV as element width and FOV is varied for 6 element array at R= 2 (a) and R=4 (b).

Figure 3 shows the inverse maximum g-factors for the six element array at reduction factors of two and four, (a) and (b) respectively. As in the four element case the minimal g-factors occurred with the maximum mean SNR over the FOV. The optimal coil widths are the same at either reduction factor though the range of acceptable FOV is significantly diminished for the R=4 case. At the higher reduction factor, smaller FOVs are unusable. It is interesting to note that in this case, a local maximum in g-factor occurs when the SNR at the center voxel of the FOV is maximized. Also, at R=2, the four element array out performs the six element array over a broader range of FOV.

DISCUSSION:

These results show that optimal g-factor performance is achieved when the mean SNR over the desired FOV is maximized by using the appropriate element. This element width remains the same at higher reduction factors while the range of acceptable FOV dimensions is reduced. The results also show that the even when not optimal, the array performance can be acceptable over a broad region making it practical for many imaging applications.

REFERENCES:

- [1] Weiger, Pruessmann, et. al.; MRM 45:495-504 (2001).
- [2] de Zwart, Leden, Kellman, et al; MRM 47:1218-1227 (2002).
- [3] Wiesinger, Boesiger, Pruessmann; MRM 52:376-390 (2004).
- [4] Reykowski, Schnell, Wang; Proc. 10th ISMRM, Honolulu, 2002, p. 2385.